Indirect Flow Rate Estimation of the NEDO PI Gyro Pump for Chronic BVAD Experiments

Daisuke Ogawa,*|| Makoto Yoshizawa,† Akira Tanaka,‡ Ken-ichi Abe,§ Paul Olegario,* Tadashi Motomura,|| Hisashi Okubo,|| Takeshi Oda,|| Toshiya Okahisa,|| Stephen R. Igo,|| and Yukihiko Nose||

In totally implantable ventricular assist device systems, measuring flow rate of the pump is necessary to ensure proper operation of the pump in response to the recipient's condition or pump malfunction. To avoid problems associated with the use of flow probes, several methods for estimating flow rate of a rotary blood pump used as a ventricular assist device have been studied. In the present study, we have performed a chronic animal experiment with two NEDO PI gyro pumps as the biventricular assist device for 63 days to evaluate our estimation method by comparing the estimated flow rate with the measured one every 2 days. Up to 15 days after identification of the parameters, our estimations were accurate. Errors increased during postoperation days 20 to 30. Meanwhile, their correlation coefficient *r* was higher than 0.9 in all the acquired data, and estimated flow rate could simulate the profile of the measured one. *ASAIO Journal* 2006; 52:266–271.

In cardiac patients, ventricular assist devices (VADs) have been developed and clinically applied for many years. Recently, totally implantable VAD systems have been used to improve a patient's quality of life. In such systems, the pump flow rate provides important information for proper pump operation in response to the recipient's condition or pump malfunction.

Usually, ultrasound and electromagnetic flow probes are used for monitoring; however, these sensors are sometimes too bulky for implantation and require additional power consumption. To avoid such problems, methods for estimating flow rate of the rotary blood pump used as a VAD have been studied.[1–5] These methods can be realized by processing the rotational speed of the impeller and power consumption of the actuator, which are easy to measure. An estimation method with an autoregressive exogenous (ARX) model also has been developed, and studies have demonstrated its capability to replace the flow meter in a mock circulatory system and acute animal experiments.[6,7]

To apply this method to clinical use, the evaluation in long-term use *in vivo* is necessary, because the time-varying condition of the circulatory system may affect the accuracy of the estimation. Ayre *et al.*[8] reported a successful result in long-term experiments but concluded that the result depended on the flat P-Q curve in the static characteristic of the pump. This implies that evaluation with other pumps should be done if we apply this method to other pumps. Tsukiya *et al.*[9] succeeded in estimating waveforms and mentioned that the method of suppressing noise in the motor current is desired. Neither of these studies reported the chronic change in the accuracy of the estimated flow rate. Other methods[4,5] were tested only in the mock circulation or acute experiment; thus, more tests in practical situations should be performed.

This author's research group developed a much smaller centrifugal pump to make it more implantable[10]; however, the characteristics of the small implantable pumps may be so different from those of other traditional pumps that it is necessary to ascertain whether this method of estimating flow rate is still valid for long-term implantation in animals. In the present study, a long-term animal study was performed with two implanted NEDO PI pumps (**Figure 1**) for 63 days, to compare the estimated flow rate with the measured flow rate in terms of the average value and similarity of the waveform.

Materials and Methods

Estimation Using ARX Model

The flow rate estimation method is based on the method proposed by Yoshizawa *et al.*[6] To correlate flow rate with rotational speed, supplied power, and other indexes, an ARX model was used given by:

$$y(k) + \sum_{i=1}^{L} a_i y(k-i) = \sum_{j=1}^{3} \sum_{i=0}^{M_j} b_{ij} u_j(k-i) + w(k) \qquad (1).$$

Inputs u_j (k) and output $y(k)$ are written as $[u_1 u_2 u_3] = [VI/N\ N\ K]$, and $Q(k)$, where $Q(k)$, I, N are flow rate, electric current, and rotational speed, respectively. k is a notation of the discrete time. $w(k)$ is the residue assumed to be white noise. V is a constant voltage of 15 V. The first and second terms in inputs, VI/N and N, were derived from the static characteristic of the pump and the circulatory system.[5] With these terms, the flow rate curve can be represented in a practical range. On the other hand, in cases where the VAD drains blood from the left ventricle, pulsatile movement of the left ventricle changes the preload of the pump. The static model cannot represent this dynamic characteristic. We replaced each term in the static characteristic with time series data and obtained the ARX model, which can represent the dynamic characteristic. With this method, a waveform that reflects the dynamics can be simulated more precisely.

The third term K is given by

From the *Graduate School of Engineering, Tohoku University, Sendai, Japan; †Information Synergy Center, Tohoku University, Sendai, Japan; ‡Faculty of Symbiotic Systems Science, Fukushima University, Fukushima, Japan; §College of Engineering, Nihon University, Koriyama, Japan; ||Michael E. DeBakey Department of Surgery, Baylor College of Medicine, Houston, Texas.

Submitted for consideration August 2005; accepted for publication in revised form February 2006.

Reprint requests: Dr. Yukihiko Nosé, Michael E. DeBakey Department of Surgery, Baylor College of Medicine, One Baylor Plaza, Houston, TX 77030.

DOI: 10.1097/01.mat.0000219066.21197.34

Figure 1. NEDO PI centrifugal pump (height of the housing: 37 mm, diameter: 55 mm).

$$K(k) = \frac{\sum_{i=1}^{n} N(k-i+1)}{\sum_{i=1}^{n} VI(k-i+1)} \quad (2)$$

and represents a steady-state gain from supplied power to rotational speed. The steady-state gain K was introduced to compensate for changes in the physiological condition such as viscosity of blood; for example, when the viscosity of blood increases, then the actuator needs more power consumption to keep the same level of flow rate. Meanwhile, power consumption increases when the flow rate is larger. These two facts mean that we cannot judge the change in flow rate only with the power consumption. To detect the change in viscosity independently, our method uses the ratio between the rotational speed and power consumption. Effectiveness of this term has been proven in the previous studies.[6,7] Taking into account the sampling rate, the orders of the model L, M_j, and n in this paper were 10, [8 8 1] and 3,000, respectively.

Figure 2 shows the idea of flow rate estimation. In practical use, $y(k)$ can be calculated with measured $u_j(k)$ and parameters a_i and b_{ij}. These parameters were identified with measured $u_j(k)$ and $y(k)$ in advance, with MATLAB R14 (Mathworks Inc., Natick, MA) and the System Identification Toolbox. The data for identification of parameters should be measured in a mock circulation, animal experiments, or during surgery.

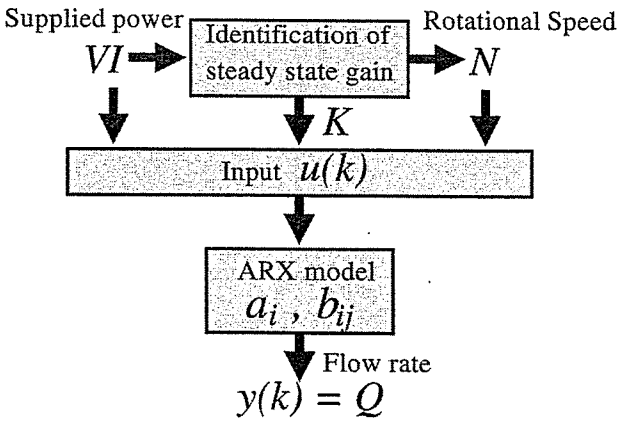

Figure 2. Idea of flow rate estimation based on supplied power and rotational speed.

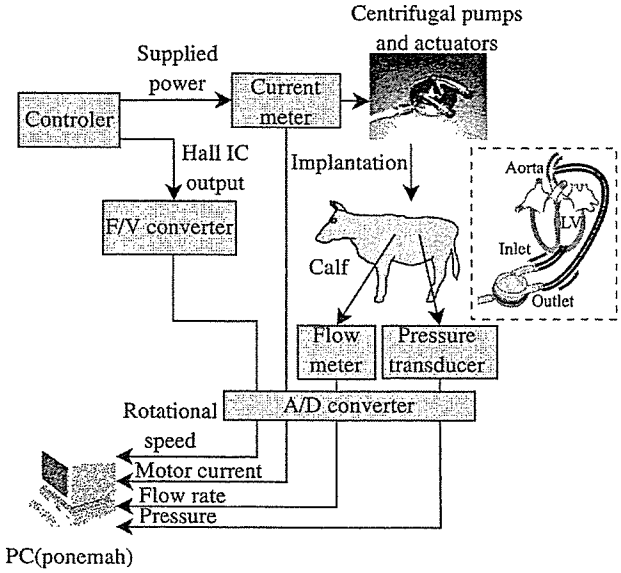

Figure 3. Experimental setup. Measurement system and connection of the LVAD and the natural heart.

Preprocessing

To eliminate noise and unfavorable components in electric current waveform, the wavelet filtering method was applied. Wavelet decomposition with bi-orthogonal function was applied to the current waveform; then, the detail coefficients smaller than the threshold level were ignored, after which the current waveform was reconstructed with the same wavelet function. All calculations were performed with MATLAB R14 and the Wavelet Toolbox. The filtering was performed using the function "wden" and mother wavelet "bior4.4" in the wavelet toolbox. For details, refer to the book.[11]

At first, to improve the accuracy of the estimation, a low-pass filter (LPF) was applied to suppress a small vibration included in the electric current. However, the LPF also removed steep changes in the rising edge of the waveform and the estimation error did not decrease. For improvement, wavelet filtering was applied, which was suitable for processing nonstationary signals

Experiment

Schematic illustration of the measurement system for the animal experiment is shown in **Figure 3**. In this system, the rotational speed was manually adjusted to keep a certain level of flow rate.

Two NEDO PI pumps were implanted in a calf as the left VAD (LVAD) and the right VAD (RVAD), respectively. The calf was healthy from the beginning of the experiment to POD 61. In the LVAD, blood was drained from the left ventricular apex with a titanium tip and a cannula connected to the inlet of the pump. The outlet of the pump was grafted to the descending

aorta, as shown in **Figure 3**. An ultrasonic flow probe (Transonic. Inc, Ithaca, NY) was placed on the graft.

Flow rate, electric current, and rotational speed were measured at 1 kHz and discretized to make the sampling rate 500 Hz every 2 days while the calf was in a sitting position, except for day (POD) 19.

The care and use of the animal reported in this study were approved by the Baylor College of Medicine Animal Protocol Review Committee.

Evaluation of Estimation Method

The datasets obtained on POD 11 and 13 were used to identify the parameters of the ARX model a_i and b_{ij}. The data consist of four sets of the measured data that were obtained while the rotational speed of the left pump (N_L) was set to 1,780 rpm, 1,700 rpm (POD 11), 1,870 rpm, and 1,700 rpm (POD 13), respectively. These operating points were in the normal range on PODs 11 and 13. The length of each data measurement was 20 seconds. The average heart rate was about 90 bpm in these four sets of data, for a total of 120 cardiac cycles, which we considered an adequate amount of data for our method.

The accuracy of the estimation was evaluated with root mean square error (*r.m.s.e*), correlation (*r*) and bias (*bias*):

$$r.m.s.e. = \sqrt{\frac{1}{K_D}\sum_{k=1}^{K_D}\{y(k) - \hat{y}(k)\}^2} \tag{3}$$

$$r = \frac{\sum_{k=1}^{K_D}\{y(k) - \bar{y}\}\{y(k) - \hat{y}\}}{\sqrt{\sum_{k=1}^{K_D}\{y(k) - \bar{y}\}^2 \sum_{k=1}^{K_D}\{\hat{y}(k) - \hat{y}\}^2}} \tag{4}$$

$$\text{bias} = \hat{y} - \bar{y} \tag{5}$$

where $\hat{y}$ is the estimate of y, $\bar{y}$ is the mean value of y, $\bar{y}$ is the mean value of $\hat{y}$, and K_D is the number of data.

Results

Result of Preprocessing

Figure 4 shows the comparison between the electric current waveforms with and without preprocessing, using wavelet filtering. In the original waveform, interesting high-frequency noise components can be found. However, they were removed, and only the profile of the original waveform was obtained by the preprocessing.

Evaluation of Waveform Estimation

Figure 5(a) shows waveforms of the measured electric current, rotational speed, flow rate of the left pump, and the estimated flow rate. **Table 1** shows *r.m.s.e.*, *r*, and *bias* in this case. The representative results in the beginning, middle, and end stage of the experiment are shown in **Figure 5(b)**. An unfavorable event of reverse flow occurred on POD 17, which indicated the value of flow rate was lower than 0 l/min, thus implying that the pump was not working efficiently. **Table 1** also shows *r.m.s.e*, *r*, and *bias* in the cases of POD 17, 37, and 57.

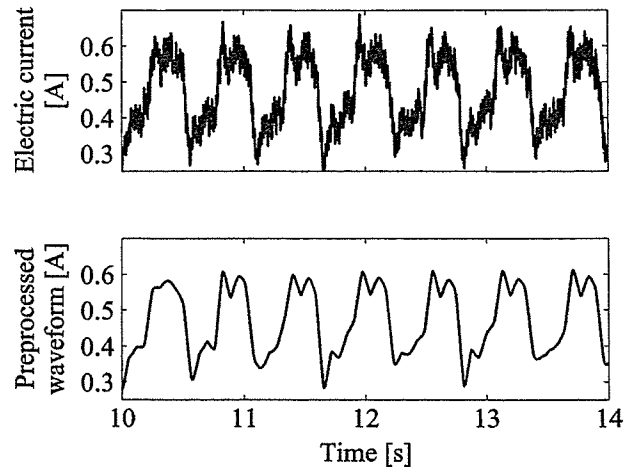

Figure 4. Original and preprocessed electric current waveforms (*top:* original waveform; *bottom:* preprocessed waveform with wavelet filtering).

Evaluation in Long-term Use

Figure 6 shows the trend of *r.m.s.e.*, *r*, and *bias* during the experiment. This figure also shows the comparison between two kinds of preprocessing, which were done by the Butterworth LPF (cutoff frequency: 400 Hz) and the wavelet filter. In the case of the LPF, the orders of the model L, M_j, and n were 0, [5 5 1], and 3,000, respectively. These values are determined by trial and error, avoiding the divergence of the estimated value. In the beginning of the experiment, *r.m.s.e.* and *bias* were not so large. After that, they tended to increase as the days passed. Meanwhile, r was higher than 0.90 in all the datasets. Wavelet filtering made r close to 1.0 and slightly improved *r.m.s.e.* and *bias*.

Rotational speed N was manually changed to keep a certain level in flow rate during the experiment. The trend of the rotational speed and pump flow during the experiment is shown in **Figure 7**. As references, the trend of physiological data (aortic pressure; AoP, and total flow measured at the pulmonary artery) and gain K are shown in **Figure 8**.

Discussion

Evaluation of Waveform Estimation

Figures 5(a) and (b) show that the estimated flow rate could simulate the profile of the measured one with good accuracy. As shown in **Figure 7**, r was high enough throughout the experiment, and wavelet filtering improved the accuracy of the estimation.

Previous studies[12] mentioned that electric current was affected by change in preload. This is the origin of the oscillation in the electric current. Meanwhile, the impeller of the NEDO PI pump levitated by hydraulic force,[13] and thus, the impeller swung periodically, which might be the reason for the small vibration in the electric current waveform. Preprocessing with wavelet transform could remove only the small vibration in waveforms without phase delay and preserve smooth changes, which was necessary to simulate the measured flow rate. This was probably the reason

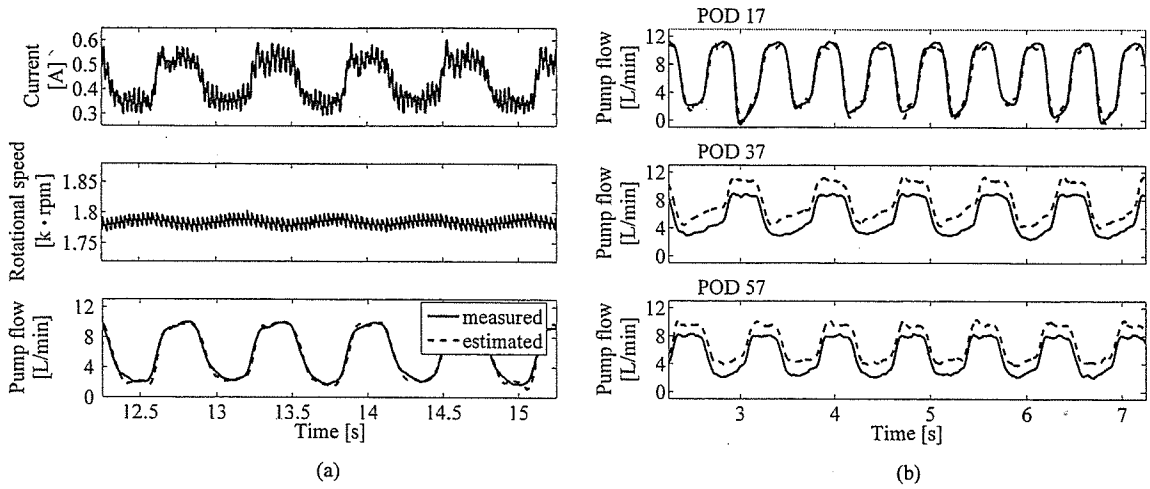

Figure 5. Comparison between the measured and the estimated flow rate (*solid line:* the measured waveform; *dotted line:* the estimated waveform). **(a)**, Pump flow and other measured data on POD 11; **(b)**, the measured and the estimated flow rate on POD 17, 37, and 57.

why the correlation *r* became higher when wavelet preprocessing was applied.

Evaluation in Long-term Use

Figure 6 shows that the correlation between the measured and the estimated waveforms was high enough during the experiment. However, *r.m.s.e.* and *bias* became gradually larger in the last stage of the experiment. This result suggested that the method could simulate waveforms of flow rate sufficiently, but it needed an improvement to compensate for the bias error that might appear in the case of long-term use. Modification of preprocessing with wavelet filtering improved *r.m.s.e.* and *bias* a little, but their values were not yet acceptable for clinical use in which another calibration could not be performed in an implanted device.

It was revealed that the waveform of the flow rate is useful in detecting the suction,[14] and our result shows that these methods are effective even in long-term use, and estimated flow rate can be substituted. Also, the reverse flow shown in **Figure 5(b)** can also be detected with our method even in long-term use. Increase in the estimation error after POD 20 to 30 shown in **Figure 7** suggested that the increase was due to several reasons.

The first possible reason was the change in the operating point of the pump. In this experiment, flow rate decreased slightly as days passed by, so rotational speed was also con-

Table 1. *r.m.s.e.*, *r*, and *bias* in Figure 5 and Figure 6

POD	*r.m.s.e.* [l/min]	*r*	*bias* [l/min]
11	0.59	0.981	0.01
17	0.42	0.994	−0.20
37	1.91	0.986	1.87
57	1.65	0.992	1.58

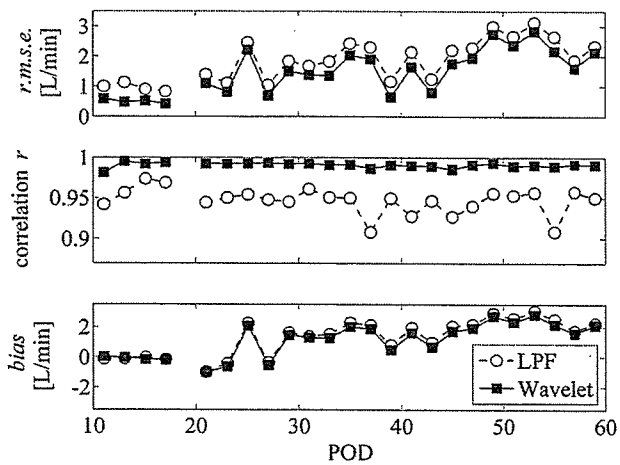

Figure 6. Trend of *r.m.s.e.*, *r*, and *bias* during the experiment (*solid line:* preprocessing with the wavelet filter; *dashed line:* low-pass filter, POD19: N/A).

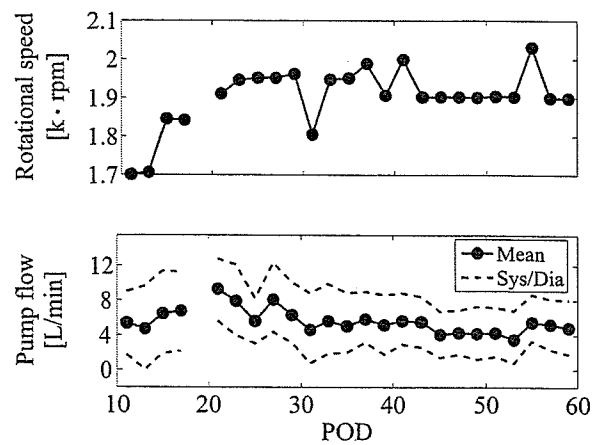

Figure 7. Trend of the operating point during the experiment (*top:* rotational speed; *bottom:* mean value of the flow rate; *dashed line* shows the peak value in systole/diastole).

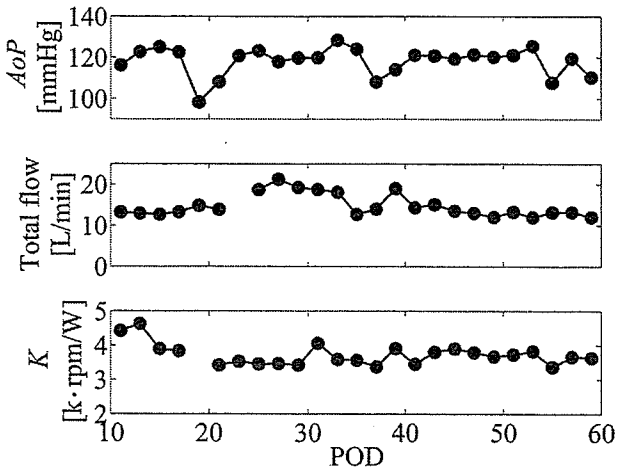

Figure 8. Trend of the average value of physiological data and gain *K* during the experiment (*top:* aortic pressure; *middle:* total flow measured at pulmonary artery; *bottom:* gain *K*).

trolled manually to keep a certain level of flow rate, as shown in **Figure 8**.

The second reason was mild intima formation at the outflow graft, which was found in the operation to wean the pumps on POD 63. Judging from the decrease in the amplitude of flow rate as shown in **Figure 7** and the change in its waveform, it could be speculated that the intima formation caused the partial obstruction of blood flow. The fact that a certain level of pump flow could be maintained throughout the experiment means this dimensional change due to intima formation was not critical for the VAD system.

In addition, the implantation of the VAD is so invasive that drastic change in physiological condition, such as vascular resistance and compliance, and regulation of the flow rate or pressure by the nervous system is possible. This is also not negligible. These problems can be avoided if we have enough data that include the wide range of operating points and various output resistances.

Limitation

This experiment was performed with a healthy calf, but usually the VAD is implanted, not in a healthy person but in a patient in abnormal condition. An experiment with an animal with low cardiac function is preferred. However, such a condition is very difficult to prepare. Analysis in the interaction between the natural heart and the VAD1[2,15] will be helpful to clarify the effect of the cardiac function against the accuracy of the estimation and improve the estimation method.

In this experiment, the data to identify the parameters of the estimator was obtained on PODs 11 and 13. In clinical use, however, it is impossible to measure flow rate after the implantation. The data used for identification should be obtained during surgery. It is desirable that generalized parameters for the estimation are approximated before the implantation. In addition, if a mock circulatory system could be built that simulates the physiological condition shown in these results, the system would also help to identify parameters more quickly and easily. However, even if such a precise mock system could be realized, the system would no longer be useful once the physiological condition varies. This is because online identification of the parameters included in the model without measuring the actual flow rate after implantation could not be performed.

Clarifying the conditions that must be included in the data for the identification of the parameters is important. Meanwhile, the data acquisition during the surgery should be as short as possible to prevent negative effect on the patient's condition. To interpolate the lack of data, some technique such as fuzzy logic or artificial neural networks will be helpful.

Conclusion

The flow estimation method was evaluated with the data acquired from a chronic animal experiment. Estimation with good accuracy was confirmed until 15 days after the identification of the parameters. However, *r.m.s.e.* and *bias* started to increase during PODs 20 to 30, because of the change in the operating point and the partial obstruction of the cannula. This problem has to be solved by a more sophisticated method if this flow estimation method were to be used.

However, correlation *r* was higher than 0.9 in all the acquired data, and estimated flow rate could simulate the profile of a measured one throughout the experiment. This information will be useful to detect an abnormal state during physiological monitoring, which does not always need an absolute value.

Acknowledgments

This project was financially supported by the New Energy and Industrial Technology Development Organization (NEDO) under the Ministry of Economy, Trade, and Industry of Japan. D. Ogawa was supported by a grant of Tohoku University 21st COE Program: "Future Medical Engineering base on Bio-nanotechnology."

References

1. Tsukiya T, Akamatsu T, Nishimura K, *et al*: Use of motor current in flow rate measurement for the magnetically suspended centrifugal blood pump. *Artif Organs* 21: 396–401, 1997.
2. Wakisaka Y, Okuzono Y, Taenaka Y, *et al*: Development of a flow estimation and control system of an implantable centrifugal blood pump for circulatory assist. *Artif Organs* 22: 488–492, 1998.
3. Ayre PJ, Vidakovic SS, Tansley GD, *et al*: Sensorless flow and head estimation in the VentrAssist rotary blood pump. *Artif Organs* 24: 585–588, 2000.
4. Kitamura T, Matsushima Y, Tokuyama T, *et al*: Physical model-based indirect measurements of blood pressure and flow using a centrifugal pump. *Artif Organs* 24: 589–593, 2000.
5. Funakubo A, Ahmed S, Sakuma I, Fukui Y: Flow rate and pressure head estimation in a centrifugal blood pump. *Artif Organs* 26: 985–990, 2002.
6. Tanaka A, Yoshizawa M, Abe K, *et al*: In vivo test of pressure head and flow rate estimation in a continuous-flow artificial heart. *Artif Organs* 27: 99–103, 2003.
7. Yoshizawa M, Sato T, Tanaka A, *et al*: Sensorless estimation of pressure head and flow of a continuous flow artificial heart based on input power and rotational speed. *ASAIO J* 48: 443–448, 2002.
8. Ayre PJ, Lovell NH, Woodard JC: Non-invasive flow estimation in

an implantable rotary blood pump: a study considering non-pulsatile and pulsatile flows. *Physiol Meas* 24: 179–189, 2003.
9. Tsukiya T, Taenaka Y, Nishinaka T, *et al*: Application of indirect flow rate measurement using motor driving signals to a centrifugal blood pump with an integrated motor. *Artif Organs* 25: 692–696, 2001.
10. Nose Y, Furukawa K: Current status of the gyro centrifugal blood pump: development of the permanently implantable centrifugal blood pump as a biventricular assist device (NEDO Project). *Artif Organs* 28: 953–958, 2004.
11. *Wavelet Toolbox* for use with MATLAB©, The Mathworks Inc; 2000.
12. Takahashi K, Uemura M, Watanabe N, *et al*: Estimation of left ventricular recovery level based on the motor current waveform analysis on circulatory support with centrifugal blood pump. *Artif Organs* 25: 713–718, 2001.
13. Asai T, Watanabe K, Ito S, *et al*: Real-time studies of the pivot bearings in the NEDO gyro PI-710 centrifugal blood pump. *Artif Organs* 28: 899–903, 2004.
14. Vollkron M, Schima H, Huber L, *et al*: Development of a suction detection system for axial blood pumps. *Artif Organs* 28: 709–716, 2004.
15. Nakata K, Shiono M, Akiyama K, *et al*: The estimation of cardiac function from the rotary blood pump. *Artif Organs* 25: 709–712, 2001.

Brief Episode of Myocardial Ischemia Before Prolonged Ischemia Attenuates Cardiac Sympathetic Nerve Injury

Teruo Nakadate, MD; Takashi Nozawa, MD; Akira Matsuki, MD; Makoto Nonomura, MD; Norio Igarashi, MD; Akihiko Igawa, MD; Hiroshi Inoue, MD

Circulation Journal
Vol. 70 No. 7 July 2006
(Pages 919–925)

Circ J 2006; **70:** 919–925

Brief Episode of Myocardial Ischemia Before Prolonged Ischemia Attenuates Cardiac Sympathetic Nerve Injury

Teruo Nakadate, MD; Takashi Nozawa, MD; Akira Matsuki, MD; Makoto Nonomura, MD; Norio Igarashi, MD; Akihiko Igawa, MD; Hiroshi Inoue, MD

Background The aim of this study was to investigate the effects of brief ischemia before prolonged ischemia on cardiac sympathetic neural function. Brief ischemia inhibits the sympathetic neural release of norepinephrine (NE) during subsequent sustained ischemia. However, whether it can attenuate the neural function after sustained ischemia remains unknown.

Methods and Results Sympathetic neural function was assessed using ^{123}I-metaiodobenzylguanidine (MIBG) in patients who with (Group I) or without angina (Group II) within 3 days prior to acute myocardial infarction. In the rat experiment, cardiac interstitial NE (iNE) with or without pretreatment of 5-min coronary ligation was determined during a 30-min occlusion. Differences between MIBG and Thallium-201 for the total defect score were significantly greater in Group II than in Group I (6.1±4.0 vs 0.4±4.4). Levels of iNE were less in rats with a 5-min pretreatment (7.3±2.3 vs 18.6±5.9 $\times 10^3$ pg/ml, $p<0.01$) and MIBG uptake of ischemic region was greater (0.061±0.029 vs 0.031±0.011 %kg dose/g, $p<0.05$) compared with rats without the pretreatment.

Conclusion A brief episode of ischemia attenuates the sympathetic neural injury caused by subsequent prolonged ischemia and this protective effect is associated with attenuation of NE release during the prolonged ischemia. (*Circ J* 2006; **70:** 919–925)

Key Words: Arrhythmia; Myocardial infarction; Nervous system; Norepinephrine; Nuclear medicine

A brief episode of transient myocardial ischemia protects the myocardium against subsequent prolonged ischemia[1] and is known as ischemic preconditioning (PC). Previous human and animal studies of PC have primarily focused on reduction of infarct size, but recent animal studies have demonstrated that a brief episode of ischemia reduces norepinephrine (NE) release during the following prolonged ischemia[2,3] This reduction of NE release may reflect attenuation of sympathetic neuronal dysfunction caused by the sustained ischemia (ie, neural PC), because the nonexocytotic NE release that occurs during ischemia is a consequence of energy starvation of the sympathetic nerve terminals[4,5] Miyazaki and Zipes demonstrated that PC preserved the efferent sympathetic and vagal responses, as assessed by measuring effective refractory periods during coronary artery occlusion in dogs[6] However, it remains unknown whether the attenuation of sympathetic neural dysfunction could be induced by a transient ischemic attack before the onset of myocardial infarction (MI) in human hearts, and whether the attenuated NE release during sustained ischemia can lead to preservation of neural function. Accordingly, the present study was performed to compare the extent and severity of cardiac sympathetic neural dysfunction associated with acute MI in patients with and without transient ischemia before the onset of MI, using a radiotracer of ^{123}I-metaiodobenzylguanidine (MIBG). Furthermore, animal studies were conducted to elucidate the relationship between neural NE release during sustained ischemia and sympathetic neural function.

(Received February 28, 2006; revised manuscript received April 11, 2006; accepted April 20, 2006)

The Second Department of Internal Medicine, University of Toyama, School of Medicine, Toyama, Japan

Mailing address: Takashi Nozawa, MD, The Second Department of Internal Medicine, University of Toyama, School of Medicine, 2630 Sugitani, Toyama 930-0194, Japan. E-mail: tnozawa@med.u-toyama.ac.jp

Methods

Clinical Study

Thirty patients who experienced a first acute MI were enrolled. All patients except 2 had ST elevation. Patients with multivessel disease, that is, those with significant coronary artery narrowing (% diameter ≥70%) in addition to the culprit region of MI, or with prior MI, were excluded. Primary percutaneous transluminal coronary angioplasty (PTCA) was performed in 20 patients and thrombolytic therapy in 3 patients. Patients were divided into 2 groups: Group I had angina within 3 days before the onset of MI, and Group II did not have angina prior to MI.

All patients gave consent to participate in this study.

^{123}I-MIBG and Thallium-201 (^{201}Tl) Imaging

^{123}I-MIBG imaging was performed in overnight fasted patients, 2–3 weeks after the onset of MI. Planar and single photon emission computed tomography (SPECT) images were acquired with a scintillation camera (CA-9300 A/DI, Toshiba, Tokyo, Japan) at 15 min (early) and 180 min (delayed) after injection of 111 MBq of ^{123}I-MIBG. The reconstructed tomographic data were displayed in horizontal long-axis, vertical long-axis, and short-axis slices with a 6.4 mm thickness. None of the study patients had received reserpine, tricyclic antidepressants, or other drugs that could interfere with ^{123}I-MIBG imaging. Exercise or dipyridamole stress ^{201}Tl imaging with the injection of 111 MBq of ^{201}Tl-chloride was performed within 1 week of

Table 1 Patient Characteristics of Groups I and II

	Group I (n=13)	Group II (n=17)
Age (years)	62±10	66±10
Male	13 (100%)	12 (71%)
Diabetes mellitus	2 (15%)	7 (41%)
Primary PTCA	9 (69%)	11 (65%)
Thrombolytic therapy	1 (8%)	2 (12%)
Infarct location		
Anteroseptal	5 (38%)	9 (53%)
Inferior	4 (31%)	5 (29%)
Other	4 (31%)	3 (18%)
TIMI flow		
0–1	9 (69%)	6 (35%)
2–3	4 (31%)	11 (65%)
Collateral index		
0–1	10 (77%)	14 (82%)
2–3	3 (23%)	3 (18%)
LVDd (mm)	51.8±4.3	52.2±7.0
LVEF	0.52±0.08	0.50±0.13

Data are mean±SD or (%).
PTCA, percutaneous transluminal coronary angioplasty; TIMI, Thrombolysis in Myocardial Infarction[10]; Collateral index, collateral flow was assessed by the Rentrop index[11]; LVDd, left ventricular end-diastolic dimension; LVEF, left ventricular ejection fraction.

the MIBG study. Early and delayed ^{201}Tl images were collected as for the MIBG images.

Data Analysis

Both MIBG and ^{201}Tl early images were visually assessed by 2 experienced nuclear cardiologists who had no knowledge of the clinical data. The 17-segment model of the left ventricle (LV) was used; each of 2 short-axis slices, the 4th and 9th slices from the apex, were divided into 8 segments, in addition to the apical segment of the horizontal long axis. Each segment was scored using a 5-point scoring system: normal (0), mildly reduced (1), moderately reduced (2), severely reduced (3), and absent uptake (4). The sum of the defect score (DS), ie, total DS (TDS), the difference in DS between ^{123}I-MIBG and ^{201}Tl (ΔDS), and the number of segments showing ΔDS ≥2 were determined.

Quantitative analysis of the SPECT data was then performed. Polar maps were divided into 24 segments and the percentage activity of ^{201}Tl and of ^{123}I-MIBG of each segment relative to the maximum LV count was determined. The ^{201}Tl and ^{123}I-MIBG polar maps were compared with those obtained from healthy control subjects (27 subjects for ^{201}Tl images, mean age 64±17 years; 21 subjects for ^{123}I-MIBG images, mean age 57±17 years). A segment was considered abnormal if the activity was more than 2 standard deviations (SD) below the mean activity for the corresponding segment in the healthy subjects.

24-h ECG Recording

Between 7 and 21 days after the onset of MI a 24-h ECG recording was performed in 10 of 13 patients in Group I and 15 of 17 patients in Group II. The ECG was analyzed using a Holter analysis system (DMW-900, Fukuda Denshi, Tokyo, Japan). The frequency of repetitive ventricular premature contractions (VPCs; ie, paired VPCs or more) was determined.

Animal Studies

All animal experiments were in accordance with the guidelines for animal experimentation and were approved by University of Toyama.

Animal Preparation Male Wistar rats weighing 300–350 g each were used for induction of myocardial ischemia as described previously[7] Briefly, under ether anesthesia, a left thoracotomy was performed to expose the heart. The left coronary artery was ligated 2–3 mm from its origin with a 5-0 Prolene suture (Ethicon Inc, Somerville, NJ, USA) for 30 min and then the ligature was released (non-PC group). In the PC group, a single 5-min coronary ligation followed by a 5-min reperfusion was conducted before the 30-min ligation.

Rat MIBG Study ^{131}I-MIBG autoradiography of the rat heart was performed as described previously[7] Briefly, 3 days after the induction of myocardial ischemia, 1.85 MBq of ^{131}I-MIBG (radiochemical purity >98%, specific activity 7.4 GBq/mg, Daiichi Radioisotope Laboratory, Chiba, Japan) was injected via the external jugular vein under pentobarbital anesthesia (30 mg/kg, ip). The heart was removed 3 h later. Serial 20-μm thick transverse sections were prepared and autoradiography was performed on an imaging plate (BAS-UR, Fuji Film, Tokyo, Japan) for 6 h.

To evaluate the myocardial accumulation of ^{131}I-MIBG, the autoradiographic images were analyzed using a computer-assisted imaging-processing system (BAS3000, Fuji Film, Tokyo, Japan) as described previously[7] The circumference of the LV was divided into 6 equal segments at the level of papillary muscles, and the ischemic region (IR) was put on the LV anterior segment and the remote region (RR), the interventricular septum, as described in the previous study[8] The myocardial tracer uptake in IR and RR was normalized as a percentage of the administered dose per gram of heart tissue (%kg dose/g) using ^{131}I-labeled graded standards.

Cardiac Microdialysis Wistar rats were anesthetized with pentobarbital sodium (30 mg/kg, ip) followed by continuous, intravenous infusion (3 mg·kg^{-1}·h^{-1}). Body temperature was maintained with a heated pad and lamp. The heart was exposed by midline incision and a microdialysis probe was inserted into the myocardium along the left coronary artery. Both ends of the dialysis fiber (8 mm length, 0.31 mm outer diameter, 0.2 mm inner diameter, 50,000 molecular weight cutoff, PAN-130SF, Asahi Chemical, Tokyo, Japan) were connected to polyethylene tubes[9,10] The dialysis probe was perfused with Ringer's solution at a rate of 2 μl/min. For baseline sampling, dialysate sampling started 60 min after the stabilization of NE concentration of the dialysate and then the left coronary artery was ligated as described in the MIBG study. Dialysate sampling was performed between 15 and 30 min after the onset of the 30-min ligation and between 0 and 15 min after the onset of reperfusion. The NE concentration of the dialysate was measured by high-performance liquid chromatography with electrochemical detection (ECD 300, EICOM, Kyoto, Japan). After the dialysate sampling, the heart was isolated and perfused with Krebs solution and the ischemic area was determined using blue ink. Also, the position of the microdialysis probe was confirmed.

Statistical Analysis

The results are expressed as mean±SD. Variables between the 2 groups were compared with unpaired t-test. ^{131}I-MIBG accumulation and NE concentration of rat hearts were compared using ANOVA followed by the Bonferroni t-test to identify differences between the groups or between IR and RR. For comparisons between Groups I and II of the

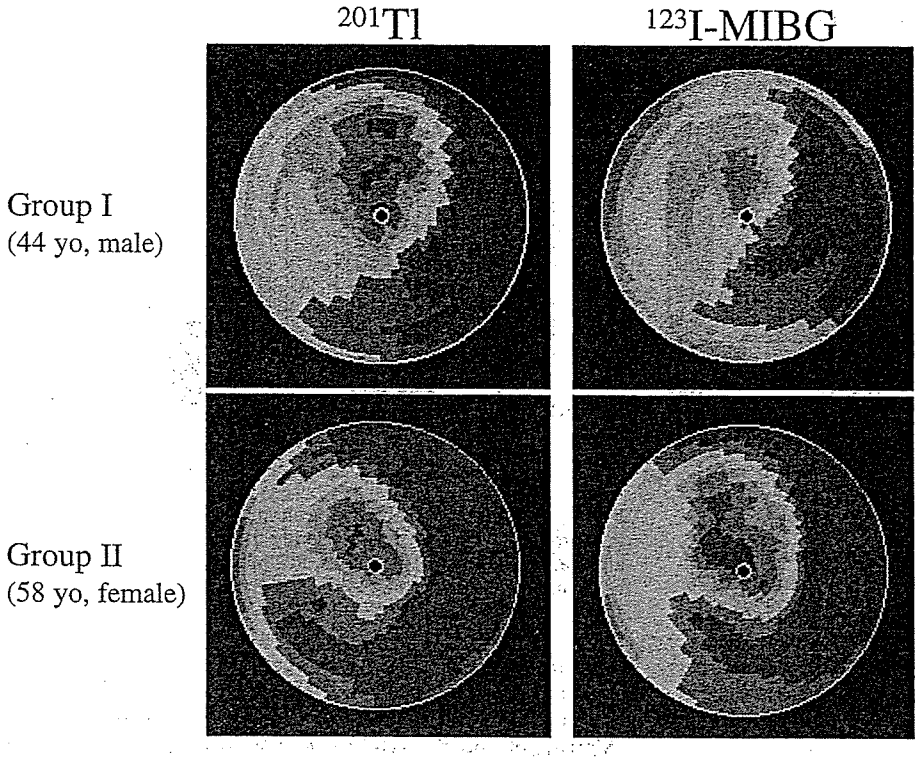

Fig 1. Representative examples of thallium-201 (^{201}Tl) and ^{123}I-metaiodobenzylguanidine (MIBG) polar maps in a 44-year-old male patient with pre-infarction angina (Group I, Upper panels) and a 58-year-old female patient without pre-infarction angina (Group II, Lower panels).

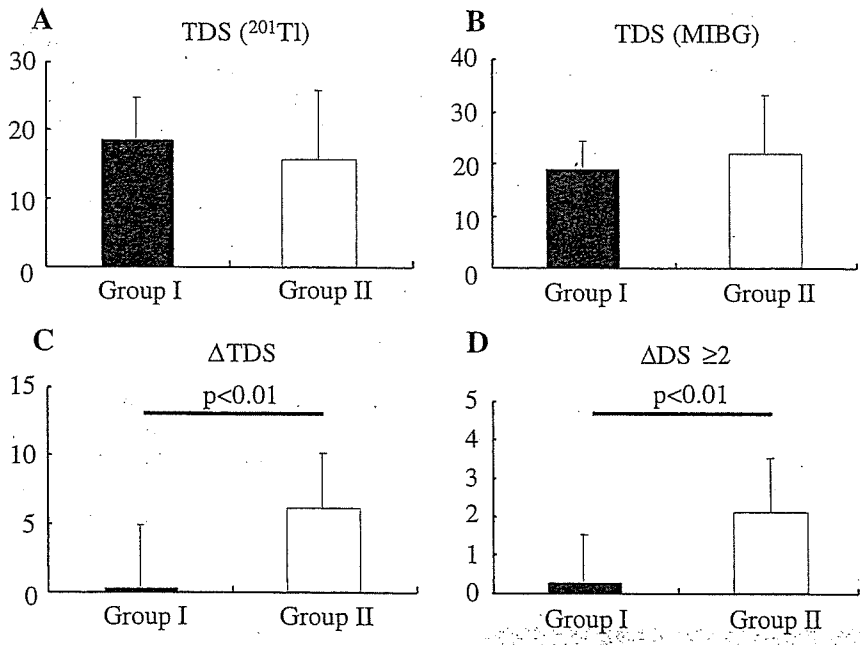

Fig 2. Comparison of thallium-201 (^{201}Tl) and ^{123}I-metaiodobenzylguanidine (MIBG) images between Groups I and II. TDS, ΔTDS, and ΔDS ≥2 indicate total defect score, differences between ^{123}I-MIBG and ^{201}Tl in the TDS, and the number of segments having a difference of the defect score ≥2, respectively.

categorical variables and the frequency of patients having repetitive VPCs, the chi-square test or Fisher's exact test was used as appropriate. A p-value less than 0.05 was considered statistically significant.

Results

Clinical Study

Patient Characteristics There were no significant differences between Group I and Group II in the number of patients with diabetes mellitus or patients treated with primary PTCA (Table 1). Primary PTCA was successfully performed in all patients. The infarct location and LV function before hospital discharge were comparable between the 2 groups. Neither the antegrade flow of culprit lesion (ie, the Thrombolysis in Myocardial Infarction (TIMI) flow grade[11]) nor the collateral flow grade assessed by the Rentrop index[12] were significantly different between the 2 groups; however, these indices were evaluated in the chronic stage before hospital discharge in 7 patients who had not undergone primary PTCA or thrombolytic therapy in the acute stage.

In Group II, the ^{123}I-MIBG images had a larger area of reduced tracer uptake than the corresponding ^{201}Tl images,

Table 2 Patient Characteristics and Ventricular Arrhythmias in Patients Undergoing 24-h ECG Recording

	Group I (n=10)	Group II (n=15)
Age (years)	64±8	65±9
LVEF	0.50±0.09	0.51±0.11
Medications		
β-blockers	7 (70%)	9 (60%)
Ca antagonists	3 (30%)	4 (27%)
ACE inhibitors	9 (90%)	11 (73%)
Anti-arrhythmic drugs	0 (0%)	1 (7%)
Repetitive VPCs	1 (10%)	8 (53%)*
Ventricular tachycardia	0 (0%)	3 (20%)

Datas are mean±SD or (%).
LVEF, left ventricular ejection fraction; ACE, angiotensin-converting enzyme; VPCs, ventricular premature contractions.
*p<0.05 vs Group I.

whereas in Group I the area of reduced ^{123}I-MIBG uptake was very close to that of ^{201}Tl uptake (Fig 1). On the average, the TDS of the ^{201}Tl and ^{123}I-MIBG images in Group I were not different from those in Group II (Figs 2A,B). However, the difference in the TDS between ^{123}I-MIBG and ^{201}Tl was significantly greater in Group II than in Group I (Fig 2C). Similarly, the number of segments with ΔDS between ^{123}I-MIBG and ^{201}T1 ≥2 was greater in Group II than in Group I (Fig 2D).

In the quantitative analysis, the number of abnormal segments was not significantly different between Groups I and II for either the ^{123}I-MIBG (7.6±3.5 and 9.1±4.1, respectively) or ^{201}Tl images (9.9±5.2 and 8.8±5.4, respectively). However, the difference between the abnormal MIBG and ^{201}Tl segments (ie, the number of abnormal ^{123}I-MIBG segments minus that of abnormal ^{201}Tl segments in each patient) was significantly smaller in Group I than in Group II (–2.3±3.9 vs 0.6±3.3, p<0.05). When the delayed ^{201}Tl images instead of the early images were used, similar differences between the 2 groups were seen for both the visual and quantitative analyses.

Table 2 presents the clinical characteristics of the patients who underwent 24-h ECG monitoring. There were no differences between the 2 groups in age, LV ejection fraction or medications, including β-blockers, Ca antagonists, and angiotensin-converting enzyme inhibitors. More Group II patients had repetitive VPCs than Group I patients. Three patients of Group II but none in Group I had ventricular tachycardia (≥3 consecutive VPCs).

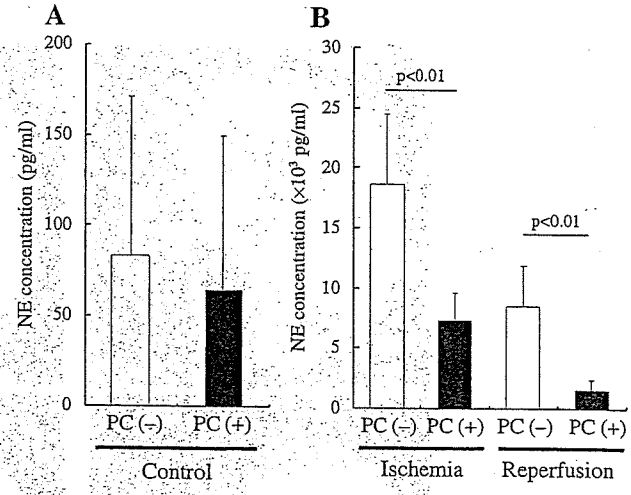

Fig 3. Cardiac interstitial norepinephrine (NE) concentration before the coronary ligation (Panel A), during the 30-min ligation, and just after reperfusion (Panel B) in rats. PC, preconditioning. The number of animals in PC(–) and PC(+) was 7 and 8, respectively.

Animal Studies

Cardiac Interstitial NE Concentration The ischemic area was similar in the PC and non-PC groups of rats (52.0±12.8 and 59.5±8.3% of LV, respectively). Before coronary ligation, there was no difference between the 2 groups in cardiac interstitial NE concentration. During the 30-min ischemia, NE concentration increased markedly in the non-PC group, but the increase was significantly attenuated in the PC group (Fig 3). After reperfusion, the NE concentration decreased in both groups but was still higher in the non-PC group than in PC group.

^{131}I-MIBG Accumulation in Rat Hearts ^{131}I-MIBG uptake in the IR was significantly greater in the PC group than in the non-PC group (Fig 4). This was also true for the ^{131}I-MIBG uptake ratio (IR/RR) (Fig 5).

Discussion

In the present study, decreases in cardiac ^{123}I-MIBG uptake relative to the corresponding ^{201}Tl images were less extensive in patients with pre-infarction angina than in those without the angina, suggesting sympathetic neural preservation by brief ischemia preceding MI. This neural PC assessed by MIBG was also revealed in the experimen-

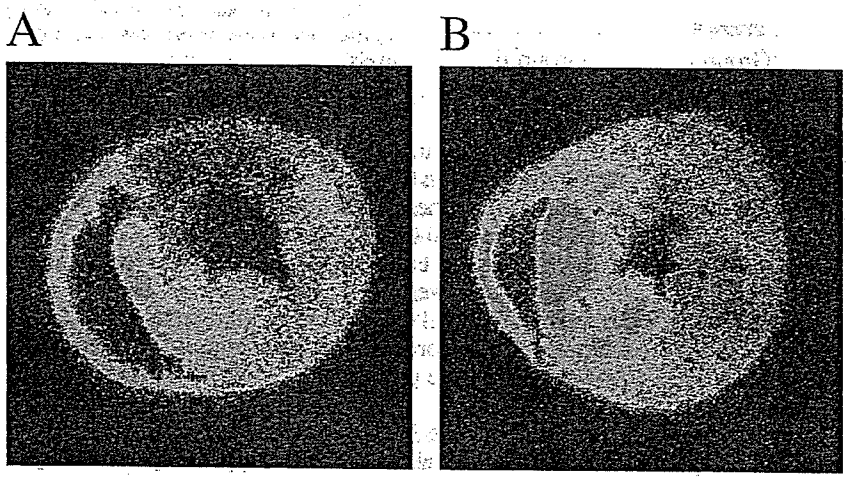

Fig 4. Representative examples of ^{131}I-metaiodobenzylguanidine (MIBG) autoradiography in rat hearts without (Panel A) and with preconditioning (Panel B). ^{131}I-MIBG uptake in the ischemic region (left ventricular free wall) was greater in the rats with preconditioning of brief ischemia.

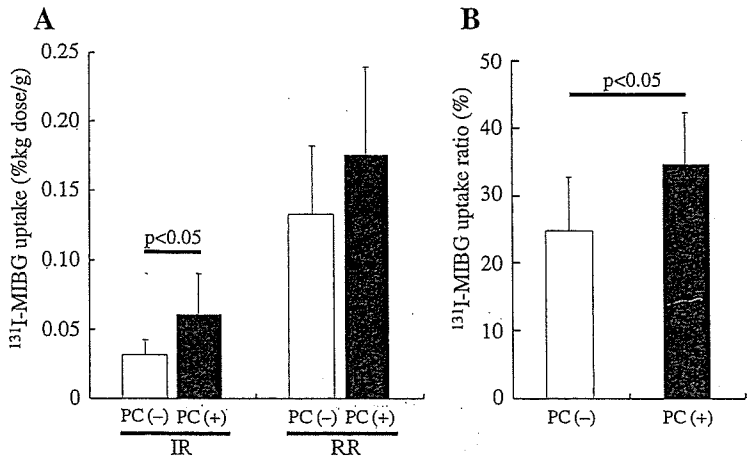

Fig 5. ^{131}I-metaiodobenzylguanidine (MIBG) uptake (Panel A) and the ratio of the uptake of the ischemic region (IR) to the remote region (RR) (Panel B) in rat hearts with or without preconditioning (PC). The number of animals in PC(–) and PC(+) was 8 and 9, respectively.

tal model of rat hearts and was preceded by attenuated NE release into the cardiac interstitial space during the coronary occlusion. To our knowledge, the present study is the first to demonstrate sympathetic neural PC in human hearts and a coupling of the attenuation of neural NE release during ischemia and preserved sympathetic neural function thereafter. We also observed that patients with pre-infarction angina had repetitive VPCs less frequently in the chronic stage before hospital discharge than those without pre-infarction angina.

Effect of PC on Neural Function

During sustained myocardial ischemia, NE release is primarily caused by a nonexocytotic mechanism, which is a consequence of energy starvation of the sympathetic nerve terminals[4,5] MIBG is an analog of NE and shares the same uptake and storage mechanism with NE at the sympathetic nerve terminals[13,14] Preserved ^{123}I-MIBG uptake in patients with pre-infarction angina may, therefore, imply less impairment of sympathetic nerve function after MI.

In the rat experiment, brief ischemia before prolonged ischemia markedly suppressed an increase in the cardiac interstitial NE levels during the subsequent prolonged ischemia, a finding consistent with previous studies[2,15] In previous studies[4,15] and our preliminary study, NE release was not induced by ischemia of short duration (<10 min) and, therefore, the reduction of NE release during subsequent, prolonged ischemia was not caused by release or degradation of NE during the brief ischemia.

The underlying mechanism of neural protection remains unclear, but the reduction of NE release implies suppression of energy starvation in the nerve terminals by PC[4] Activation of the K_{ATP} channel may be important in ischemic PC of sympathetic nerves[15–17] However, Schömig et al reported that reduced activation of the Na^+–H^+ exchange after brief ischemia may result in the suppression of NE release during subsequent, prolonged ischemia[5] Taken together, the findings suggest that the mechanism for reducing ischemia-induced NE release may involve inhibition of intracellular Na^+ accumulation. The suppression of NE release by PC might reduce NE-derived free radical formation[18,19] thereby contributing to the preservation of neural function after prolonged ischemia. Thus, in patients with pre-infarction angina the brief ischemia before MI could reduce NE release and attenuate the damage to sympathetic nerve endings.

In both humans and experimental animal studies of MI[20–22] the sympathetic nerve injury assessed by MIBG often exceeds the area of myocardial necrosis. Reduced MIBG uptake is also found in patients with angina pectoris but without MI[23–25] These observations suggest that the vulnerability of sympathetic nerves to ischemia may differ from that of myocytes. In addition to neural PC, brief ischemia before prolonged ischemia might reduce the infarct size and, therefore, may have affected the TDS for the ^{201}Tl and ^{123}I-MIBG images in the present human study. However, the present results of the human studies also suggest that the influence of brief ischemia before MI on the myocardium might be negligible or smaller than that on the sympathetic nerve terminals.

Effect of PC on Ventricular Arrhythmias

Activation of the sympathetic nervous system after MI may play an important role in arrhythmogenesis[26] In addition, heterogeneity of ventricular repolarization because of heterogeneous sympathetic innervation after MI may have a potential arrhythmogenic effect[27–29] A previous study demonstrated that ventricular arrhythmias occurring in patients who had suffered MI were associated with increased mortality during the follow-up period[30] In a multicenter study, paired VPCs after MI were associated with a more than 3-fold increase in the odds ratio of mortality compared with those with no VPC, and ventricular tachycardia with a 5- to 6-fold increase in the odds ratio[31] The peri-infarct area with normal flow tracer uptake but reduced MIBG uptake is considered to be "denervated but viable" myocardium that may be supersensitive to catecholamines, and therefore, may be arrhythmogenic[32]

Study Limitations

Some methodological limitations of this study deserve comment in the interpretion of the present results. First, tracer uptake of human hearts is often lower in the LV inferior region than in the other regions, especially with ^{123}I-MIBG imaging[33] However, the number of patients with inferior MI was not different between the 2 groups in the present study. The attenuation of reduced ^{123}I-MIBG uptake compared with ^{201}Tl uptake found in patients with pre-infarction angina was observed in patients with inferior MI, as well as in those with other MI locations. Second, the TIMI flow grade before the coronary intervention was not significantly different between the 2 groups but there was a trend towards a greater number of patients with TIMI grade ≥2 in Group II (p=0.07). This antegrade flow before

coronary intervention might protect the myocardium from irreversible damage but not be sufficient to protect sympathetic neuronal function, because the sympathetic nerve is more vulnerable to ischemic injury than myocytes[23,24] This statistically insignificant difference between the 2 groups in antegrade flow might partially affect the present results.

Finally, in the human study of ^{123}I-MIBG and ^{201}Tl scintigraphy, early images were analyzed, because the early ^{123}I-MIBG image reflects the neuronal function better than the delayed image[34] and the early image of stress ^{201}Tl scintigraphy reflects the risk area of myocardial ischemia better than the delayed, redistribution image. When the delayed ^{201}Tl images were used, similar differences between ^{123}I-MIBG and ^{201}Tl images were observed in the present study. During stress ^{201}Tl scintigraphy, 2 patients of Group I and 5 patients of Group II had stress-induced ischemia in the peri-infarct region. When these patients with stress-induced ischemia were excluded, the differences between ^{123}I-MIBG and ^{201}Tl in the TDS and the number of segments with ΔDS $\geq$2 were still significantly lower in Group I than in Group II. Thus, the existence of residual ischemia might not primarily affect the present results.

In conclusion, patients with brief ischemia before MI had attenuation of sympathetic neural dysfunction, a phenomenon termed "neural PC", in association with a lower frequency of repetitive VPCs. This neural PC assessed by MIBG was also detected in experimental rat hearts and was coupled with attenuated NE release from the sympathetic nerve terminals during ischemia. Neural PC induced by a pharmacological intervention, for example, KATP channel opener or Na^+–H^+ exchange inhibitor, could inhibit the expansion of neural dysfunction, possibly leading to suppression of ventricular arrhythmias.

References

1. Murry CE, Jennings RB, Reimer KA. Preconditioning with ischemia: A delay of lethal cell injury in ischemic myocardium. *Circulation* 1986; **74:** 1124–1136.
2. Seyfarth M, Richardt G, Mizsnyak A, Kurz T, Schömig A. Transient ischemia reduces norepinephrine release during sustained ischemia: Neural preconditioning in isolated rat heart. *Circ Res* 1996; **78:** 573–580.
3. De Jong JW, Cargnoni A, Bradamante S, Curello S, Janssen M, Pasini E, et al. Intermittent vs continuous ischemia decelerates adenylate breakdown and prevents norepinephrine release in reperfused rabbit heart. *J Mol Cell Cardiol* 1995; **27:** 659–671.
4. Schömig A, Fischer S, Kurz T, Richardt G, Schömig E. Non-exocytotic release of endogenous noradrenaline in the ischemic and anoxic rat heart: Mechanism and metabolic requirements. *Circ Res* 1987; **60:** 194–205.
5. Schömig A, Kurz T, Richardt G, Schömig E. Neuronal sodium homeostasis and axoplasmic amine concentration determine calcium-independent norepinephrine release in normoxic and ischemic rat heart. *Circ Res* 1988; **63:** 214–226.
6. Miyazaki T, Zipes DP. Protection against autonomic denervation following acute myocardial infarction by preconditioning ischemia. *Circ Res* 1989; **64:** 437–448.
7. Igawa A, Nozawa T, Yoshida N, Fujii N, Inoue M, Tazawa S, et al. Heterogeneous cardiac sympathetic innervation in heart failure after myocardial infarction of rats. *Am J Physiol* 2000; **278:** H1134–H1141.
8. Kato B, Nozawa T, Igarashi N, Nonomura M, Fujii N, Igawa A, et al. Discrepant recovery course of sympathetic neuronal function and beta-adrenoceptors in rat hearts after reperfusion following transient ischemia. *J Nucl Med* 2004; **45:** 1074–1080.
9. Yamazaki T, Akiyama T, Kitagawa H, Takauchi Y, Kawada T, Sunagawa K. A new, concise dialysis approach to assessment of cardiac sympathetic nerve terminal abnormalities. *Am J Physiol* 1997; **272:** H1182–H1187.
10. Nonomura M, Nozawa T, Matsuki A, Nakadate T, Igarashi N, Kato B, et al. Ischemia-induced norepinephrine release, but not norepinephrine-derived free radicals, contributes to myocardial ischemia-reperfusion injury. *Circ J* 2005; **69:** 590–595.
11. The TIMI Study Group. The Thrombolysis in Myocardial Infarction (TIMI) trial: Phase 1 findings. *N Engl J Med* 1985; **312:** 932–936.
12. Cohen M, Rentrop KP. Limitation of myocardial ischemia by collateral circulation during sudden controlled coronary artery occlusion in human subjects: A prospective study. *Circulation* 1986; **74:** 469–476.
13. Nakajo M, Shimabukuro K, Yoshimura H, Yonekura R, Nakabeppu Y, Tanoue P, et al. Iodine-131 metaiodobenzylguanidine intra- and extravesicular accumulation in the rat heart. *J Nucl Med* 1986; **27:** 84–89.
14. Nozawa T, Igawa A, Yoshida N, Maeda M, Inoue M, Yamamura Y, et al. Dual-tracer assessment of coupling between cardiac sympathetic neuronal function and downregulation of beta-receptors during development of hypertensive heart failure of rats. *Circulation* 1998; **97:** 2359–2367.
15. Miura T, Kawamura S, Tatsuno H, Ikeda Y, Mikami S, Iwamoto H, et al. Ischemic preconditioning attenuates cardiac sympathetic nerve injury via ATP-sensitive potassium channels during myocardial ischemia. *Circulation* 2001; **104:** 1053–1058.
16. Hausser MA, de Weille JR, Lazdunski M. Activation by cromakalim of pre- and post-synaptic ATP-sensitive K^+ channels in substantia nigra. *Biochem Biophys Res Commun* 1991; **174:** 909–914.
17. Oe K, Sperlágh B, Sántha E, Markó I, Nagashima H, Foldes FF, et al. Modulation of norepinephrine release by ATP-dependent K^+-channel activators and inhibitors in guinea-pig and human isolated right atrium. *Cardiovasc Res* 1999; **43:** 125–134.
18. Albino Teixeira A, Azevedo I, Branco D, Rodrigues-Pereira E, Osswald W. Sympathetic denervation caused by long-term noradrenaline infusions; prevention by desipramine and superoxide dismutase. *Br J Pharmacol* 1989; **97:** 95–102.
19. Liang C, Rounds NK, Dong E, Stevens SY, Shite J, Qin F. Alterations by norepinephrine of cardiac sympathetic nerve terminal function and myocardial beta-adrenergic receptor sensitivity in the ferret: Normalization by antioxidant vitamins. *Circulation* 2000; **102:** 96–103.
20. Iwasaki T, Suzuki T, Tateno M, Sasaki Y, Oshima S, Imai S. Dual-tracer autoradiography with thallium-201 and iodine-125-metaiodobenzyl- guanidine in experimental myocardial infarction of rat. *J Nucl Med* 1996; **37:** 680–684.
21. Dae MW, Herre JM, O'Connell JW, Botvinick EH, Newman D, Munoz L. Scintigraphic assessment of sympathetic innervation after transmural versus nontransmural myocardial infarction. *J Am Coll Cardiol* 1991; **17:** 1416–1423.
22. Matsunari I, Schricke U, Bengel FM, Haase HU, Barthel P, Schmidt G, et al. Extent of cardiac neuronal damage is determined by the area of ischemia in patients with acute coronary syndromes. *Circulation* 2000; **101:** 2579–2585.
23. Tomoda H, Yoshioka K, Shiina Y, Tagawa R, Ide M, Suzuki Y. Regional sympathetic denervation detected by iodine 123 metaiodobenzylguanidine in non-Q-wave myocardial infarction and unstable angina. *Am Heart J* 1994; **128:** 452–458.
24. Taki J, Yasuhara S, Takamatsu T, Nakajima K, Tatami R, Ishise S, et al. Value of iodine-123 metaiodobenzyl-guanidine scintigraphy in patients with vasospastic angina. *Eur J Nucl Med* 1998; **25:** 229–234.
25. Sakata K, Iida K, Kudo M, Yoshida H, Doi O. Prognostic value of I-123 metaiodobenzylguanidine imaging in vasospastic angina without significant coronary stenosis. *Circ J* 2005; **69:** 171–176.
26. Corr PB, Gillis RA. Autonomic neural influences on the dysrhythmias resulting from myocardial infarction. *Circ Res* 1978; **43:** 1–9.
27. Inoue H, Zipes DP. Results of sympathetic denervation in the canine heart: Supersensitivity that may be arrhythmogenic. *Circulation* 1987; **75:** 877–887.
28. Dae MW, Lee RJ, Ursell PC, Chin MC, Stillson CA, Moise NS. Heterogeneous sympathetic innervation in German shepherd dogs with inherited ventricular arrhythmia and sudden cardiac death. *Circulation* 1997; **96:** 1337–1342.
29. Stanton MS, Tuli MM, Radtke NL, Heger JJ, Miles WM, Mock BH, et al. Regional sympathetic denervation after myocardial infarction in humans detected noninvasively using I-123-metaiodobenzylguanidine. *J Am Coll Cardiol* 1989; **14:** 1519–1526.
30. Bigger JT, Weld FM, Rolnitzky LM. Prevalence, characteristics and significance of ventricular tachycardia (two or more complexes) detected with ambulatory electrocardiographic recording in the late hospital phase of acute myocardial infarction. *Am J Cardiol* 1981; **48:** 815–823.

31. Bigger JT Jr, Fleiss JL, Kleiger R, Miller JP, Rolnitzky LM. The relationships among ventricular arrhythmias, left ventricular dysfunction, and mortality in the 2 years after myocardial infarction. *Circulation* 1984; **69:** 250–258.
32. Kammerling JJ, Green FJ, Watanabe AM, Inoue H, Barber MJ, Henry DP, et al. Denervation supersensitivity of refractoriness in noninfarcted areas apical to transmural myocardial infarction. *Circulation* 1987; **76:** 383–393.
33. Gill JS, Hunter GJ, Gane G, Camm AJ. Heterogeneity of the human myocardial sympathetic innervation: In vivo demonstration by iodine 123-labeled metaiodobenzylguanidine scintigraphy. *Am Heart J* 1993; **126:** 390–398.
34. Dae MW, De Marco T, Botvinick EH, O'Connell JW, Hattner RS, Huberty JP, et al. Scintigraphic assessment of MIBG uptake in globally denervated human and canine hearts-implications for clinical studies. *J Nucl Med* 1992; **33:** 1444–1450.

Influence of β-Adrenoceptor Blockade on the Myocardial Accumulation of Fatty Acid Tracer and Its Intracellular Metabolism in the Heart After Ischemia-Reperfusion Injury

Norio Igarashi, MD; Takashi Nozawa, MD; Nozomu Fujii, MD;
Takayuki Suzuki, MD; Akira Matsuki, MD; Teruo Nakadate, MD;
Akihiko Igawa, MD; Hiroshi Inoue, MD

Circulation Journal
Vol. 70 No. 11 November 2006
(Pages 1509–1514)

Circ J 2006; **70:** 1509–1514

Influence of β-Adrenoceptor Blockade on the Myocardial Accumulation of Fatty Acid Tracer and Its Intracellular Metabolism in the Heart After Ischemia-Reperfusion Injury

Norio Igarashi, MD; Takashi Nozawa, MD; Nozomu Fujii, MD; Takayuki Suzuki, MD; Akira Matsuki, MD; Teruo Nakadate, MD; Akihiko Igawa, MD; Hiroshi Inoue, MD

Background Increases in sympathetic nerve activity during ischemia may increase intracellular fatty acid (FA) accumulation via enhanced FA uptake and inhibition of β-oxidation. Therefore, the beneficial effects of β-adrenoceptor blockade on myocardial ischemic injury might result from the suppression of FA accumulation.

Methods and Results Carvedilol (1 mg/kg) or propranolol (1 mg/kg) was injected 10 min before 15-min occlusion of coronary artery in rats. Myocardial FA accumulation and intracellular metabolites of FA tracer were determined 3 days after reperfusion using ^{125}I- and ^{131}I-9-metylpentadecanoic acid (9MPA). Carvedilol significantly decreased 9MPA accumulation in both the ischemic region (IR) and non-IR, as compared with vehicle, and increased its clearance. However, the non-metabolized 9MPA fraction was not different between carvedilol- and vehicle-treated rats. Consequently, the amount of non-metabolized 9MPA in the myocardium was lower in rats treated with carvedilol than in those given vehicle. These effects of carvedilol were not different from those of propranolol.

Conclusion Beta-adrenoceptor blockade did not affect a visual assessment of the autoradiographic image of 9MPA in hearts subjected to ischemia-reperfusion, but it accelerated the clearance of 9MPA in both the IR and non-IR. The administration of β-blockade before ischemia could accelerate the recovery from ischemia-reperfusion injury by inhibiting myocardial FA accumulation before β-oxidation. (*Circ J* 2006; **70:** 1509–1514)

Key Words: β-adrenoceptor blockade; Fatty acids; Ischemia-reperfusion; Metabolism; Myocardium; Radiotracers

Much evidence has demonstrated that treatment with β-adrenoceptor blockade in patients with ischemic heart disease and chronic heart failure can improve their symptoms and prognosis. The harmful effects of adrenoceptor stimulation are related to increased oxygen consumption and enhanced free fatty acid (FFA) use secondary to elevated levels of plasma FFA and to increased intramyocardial lipolysis[1] However, it is still unclear if β-adrenoceptor blockade has a beneficial effect on the heart subjected to ischemia-reperfusion in terms of myocardial fatty acid (FA) metabolism.

Recently, branched-chain FA analogs, such as ^{123}I-15-β-methyl-p-iodophenyl-pentadecanoic acid (BMIPP) and ^{123}I-15-(p-iodophenyl)-9-methylpentadecanoic acid (9MPA), have been clinically applied to assess FA metabolism in patients with ischemic heart disease[2–6] In contrast to a straight-chain FA, methyl-branched FA analogs are expected to interfere with β-oxidation because the metabolic process requires α-oxidation before β-oxidation[7] However, previous studies[8–10] demonstrated that branched-chain FA analogs could be metabolized within the myocardium by α- and β-oxidation, and cardiac imaging using these analogs could reflect, at least in part, myocardial FA metabolism including β-oxidation. Most patients with ischemic heart disease are treated with β-adrenoceptor blockade and therefore it is important to clarify the influence of β-blockade on cardiac accumulation of the FA tracer and its intracellular metabolism. The purpose of this study was to determine the effect of carvedilol on the autoradiographic images obtained using 9MPA, as well as alterations in the intracellular oxidation of the tracer, in rat hearts after ischemia-reperfusion injury and compare it with propranolol.

(Received June 14, 2006; revised manuscript received August 29, 2006; accepted September 4, 2006)

Second Department of Internal Medicine, Faculty of Medicine, University of Toyama, Toyama, Japan

Mailing address: Takashi Nozawa, MD, Second Department of Internal Medicine, Faculty of Medicine, University of Toyama, 2630 Sugitani, Toyama 930-0194, Japan. E-mail: tnozawa@med.u-toyama.ac.jp

Methods

Experimental Animals

All animal experiments were in accordance with the guidelines for animal experimentation and were approved by the University of Toyama.

Male Wistar rats weighing 300–350 g were used for induction of ischemia-reperfusion injury as described previously[11] Briefly, under ether anesthesia, a left thoracotomy was performed to expose the heart. The left coronary artery was ligated 2–3 mm from its origin with a 5-0 Prolene suture (Ethicon Inc, Somerville, NJ, USA) for 15 min and then the ligation was released. Sham operation was performed using the same procedure except for the coronary artery ligation. The rats were divided into 4 groups: saline

Table 1 Plasma Concentrations of FFA, TG, and Glucose in the 4 Treatment Groups

	Sham (n=8)	*Vehicle (n=5)*	*Propranolol (n=8)*	*Carvedilol (n=7)*
FFA (mmol/L)	*1.03±0.15*	*0.90±0.16*	*0.89±0.20*	*0.93±0.14*
TG (mg/dl)	*31.8±9.4*	*24.2±11.7*	*35.5±9.8*	*28.1±10.9*
Glucose (mg/dl)	*122.5±21.4*	*134.1±10.6*	*120.7±18.1*	*116.4±14.3*

FFA, free fatty acids; TG, triglycerides. Mean±SD.

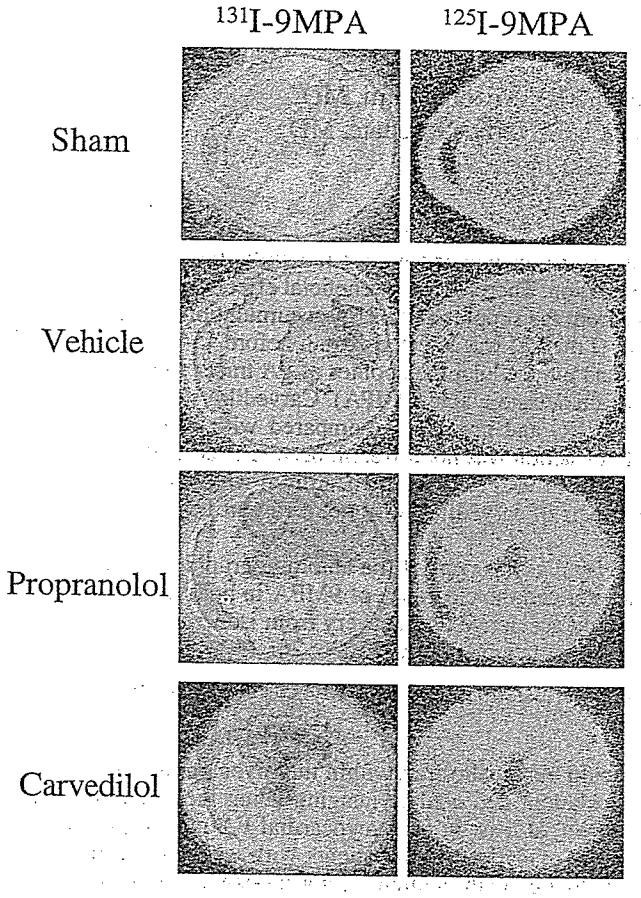

Fig 1. Representative examples of myocardial 9-methylpentadecanoic acid (9MPA) accumulation shown by dual-tracer autoradiography. ^{131}I-9MPA, images obtained 5 min after tracer injection; ^{125}I-9MPA, 60 min after injection.

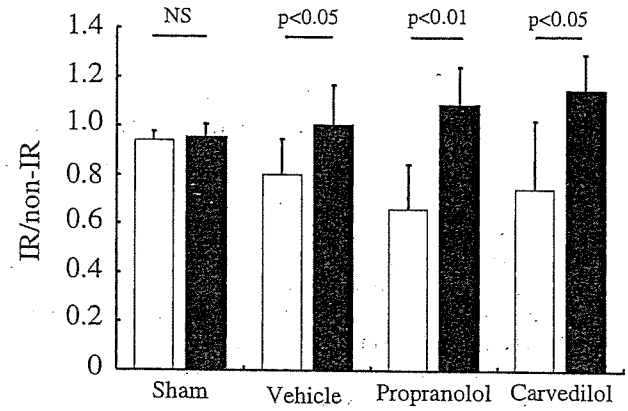

Fig 2. Nine-methylpentadecanoic acid (9MPA) accumulation ratio of the ischemic region (IR) to non-ischemic region (Non-IR) in sham-operated (n=4), vehicle (n=6), propranolol (n=6), and carvedilol rats (n=5). (Open bars) ^{131}I-9MPA accumulation ratio; (solid bars) ^{125}I-9MPA accumulation ratio. Mean+SD.

infusion (vehicle), carvedilol (1 mg/kg, iv), propranolol (1 mg/kg, iv), and sham operation. Beta-adrenoceptor blockade or saline was administered intravenously 10 min before the coronary occlusion. Cardiac dual-tracer autoradiography was performed to determine myocardial accumulation and clearance of the FA analog 3 days after the ischemic insult. In separate animals, thin-layer chromatography (TLC) was performed to determine the intracellular metabolic products of the FA analog 3 days after the ischemic insult. Cardiac dual-tracer autoradiography and TLC were performed after the animals were fasted for 24 h before the study. Blood sampling was performed during the TLC study to determine plasma concentrations of FFA, triglycerides (TG), and glucose.

FA Tracers

In the present study, myocardial FA metabolism was assessed with ^{131}I-and ^{125}I-9MPA. 9MPA was prepared and supplied by Daiichi Radioisotope Laboratory Co, Ltd (Tokyo, Japan) and its radiochemical was more than 98%, and its specific activity was 30–70 GBq/mmol.

Cardiac 9MPA Accumulation

Dual-tracer autoradiography with ^{131}I-9MPA and ^{125}I-9MPA was performed to determine the myocardial accumulation and clearance of 9MPA as described previously[10] Briefly, animals were injected intravenously with 0.74 MBq of ^{125}I-9MPA and 55 min later with 5.55 MBq of ^{131}I-9MPA. The hearts were removed 5 min after the second injection. Serial 20-μm transverse sections were prepared. The first autoradiographic exposure on an imaging plate (BAS-UR, Fuji Film, Tokyo, Japan) was carried out for 8 h to reveal ^{131}I-9MPA accumulation. The second exposure for the ^{125}I-9MPA image was initiated 75 days later following the decay of ^{131}I-9MPA activity, and required 30 days for adequate image quality. With the present doses of ^{131}I and ^{125}I, the cross-talk between the 2 tracers was less than 3%[10]

To determine the myocardial accumulation of 9MPA, the autoradiographic images were analyzed using a computer-assisted imaging-processing system (BAS3000, Fuji Film) as described previously[10] The region of interest was put on the left ventricular (LV) anterior wall (ischemic region, IR) and septal wall (non-ischemic region, non-IR) at the level of papillary muscles, and the IR was defined as one-sixth of the whole LV area around the center of ischemia on the autoradiographic image[11] The myocardial tracer uptake in the IR and non-IR was normalized as a percentage of the administered dose per gram of heart tissue (%dose/g) using ^{131}I- and ^{125}I-labeled graded standards. The clearance of 9MPA (ie, its washout rate (WR)), in the IR and non-IR

Table 2 Myocardial 9MPA Accumulation and Washout Rate in the 4 Treatment Groups

	^{131}I (%dose/g)		^{125}I (%dose/g)		WR (%)	
	IR	Non-IR	IR	Non-IR	IR	Non-IR
Sham (n=4)	6.00±1.04	6.41±1.31	2.85±0.49	3.02±0.69	52.2±6.3*	52.8±6.2
Vehicle (n=6)	4.76±0.81†	5.99±0.93‡	3.02±0.41	3.12±0.28	33.3±5.6	46.8±9.7‡
Proranolol (n=6)	3.03±1.08*	4.52±0.59*,‡	1.17±0.15*	1.10±0.22*	56.1±18.0*	75.1±7.0*,‡
Carvedilol (n=5)	2.78±0.48*	4.21±1.78*,‡	1.11±0.30*	0.96±0.24*	59.6±11.7*	73.3±12.4*,‡

WR, washout rate of 9MPA; IR, ischemic region; Non-IR, non-ischemic region.
†$p<0.01$ vs sham, *$p<0.01$ vs vehicle, ‡$p<0.05$ vs IR.

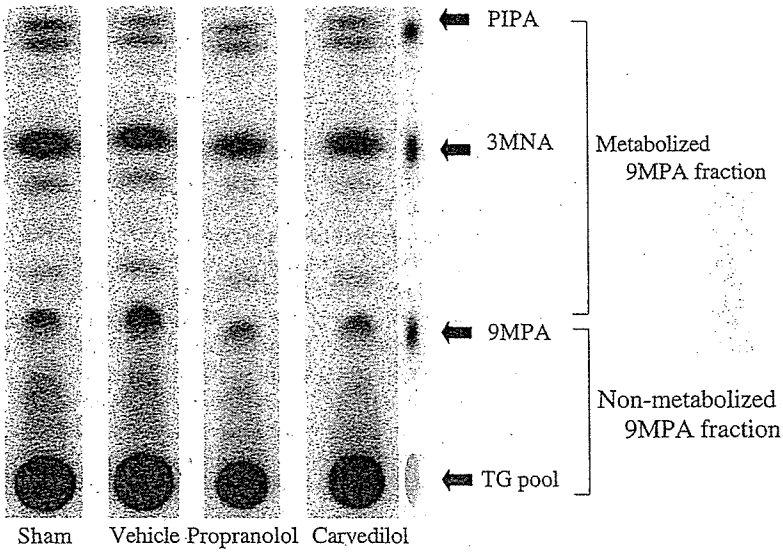

Fig 3. Representative examples of thin-layer chromatography of 9-methylpentadecanoic acid (9MPA) 3 days after reperfusion following 15-min coronary occlusion. The bottom spots are 9MPA in the triglyceride (TG) pool. The sum of radioactivity from the intermediate metabolites above 9MPA to p-iodophenyl acetic acid (PIPA) was defined as the metabolized 9MPA fraction processed by β-oxidation. 3MNA, 3-methylnonanoic acid. Samples were obtained from the ischemic region.

was calculated using the following equation:

$$WR\ (\%) = (^{131}I\ \text{uptake} - ^{125}I\ \text{uptake}) \times 100 \div ^{131}I\ \text{uptake}.$$

Analysis of 9MPA Metabolites

Lipid extraction from myocardial tissues was performed according to a modification of the method of Folch et al,[12] with the metabolic products of 9MPA being assessed by TLC. A dose of 3.7 MBq of ^{125}I-9MPA was administered intravenously under pentobarbital anesthesia. The hearts were quickly removed 5 min later and the LV tissue from the IR and non-IR was separately homogenized. The radioactivity of the 9MPA metabolites was assayed by TLC on aluminum sheets (RP-18F; Merck, Germany) in conjunction with standard lipid preparations. The metabolites of 9MPA on the aluminum sheets were exposed on the imaging plate for 14 days and quantified with a bioimaging analyzer (BAS3000). Two major metabolites of 9MPA detected on the exposed images were 3-methylnonanoic acid (3MNA) as the intermediate metabolite after 3 cycles of β-oxidation from 9MPA, and p-iodo-phenyl acetic acid (PIPA) representing the final product of 9MPA.[13]

Statistical Analysis

Data are expressed as mean ± SD. Group comparisons were made using ANOVA followed by a Bonferroni test to identify differences between the groups. Comparison between the IR and non-IR in each heart was performed by paired t-tests. A value of $p<0.05$ was considered statistically significant.

Results

Cardiac 9MPA Accumulation

None of the plasma levels of FFA, TG, or glucose differed among the 4 groups (Table 1). LV accumulation of ^{131}I- and ^{125}I-9MPA was homogeneous in the sham rats. However, in the other 3 groups (ie, vehicle, carvedilol, and propranolol groups) ^{131}I-9MPA accumulation was lower in the IR as compared with the non-IR. In contrast, ^{125}I-9MPA accumulation in the LV was relatively homogeneous in these groups, suggesting slower 9MPA clearance in the IR than in the non-IR (Figs 1,2). Carvedilol decreased ^{131}I- and ^{125}I-9MPA accumulation in both the IR and non-IR, and the WR of the tracer was significantly greater in the carvedilol group than in the vehicle group (Table 2). None of the autoradiographic indices in the rats treated with propranolol differed from those with carvedilol.

Analysis of 9MPA Metabolites

Representative examples of TLC in the IR and non-IR are shown in Fig 3. The sum of 3MNA, PIPA, and the other intermediate metabolites processed via β-oxidation was defined as the metabolized 9MPA fraction in the present study. In rats treated with vehicle, the metabolized fraction of the IR was less than that of the non-IR, and was also less than that of the sham rats (Table 3). Neither carvedilol nor propranolol affected the metabolized or non-metabolized 9MPA fraction in either the IR or non-IR.

The amount of non-metabolized 9MPA in the myocardium at 5 min after the tracer injection was calculated from the mean values of myocardial ^{131}I-9MPA accumulation de-

Table 3 Metabolized and Non-Metabolized 9MPA Fractions in the IR and Non-IR of the 4 Treatment Groups

	Non-metabolized fraction (%)		Metabolized fraction (%)	
	IR	Non-IR	IR	Non-IR
Sham (n=8)	40.0±6.9	39.2±5.1	60.0±7.2	60.8±5.3
Vehicle (n=5)	53.8±2.3*	46.0±6.6‡	46.2±2.5*	54.0±7.0‡
Propranolol (n=8)	48.9±4.5*	41.0±7.1‡	51.1±4.6*	59.0±7.3‡
Carvedilol (n=7)	51.6±1.6*	44.8±2.0‡	48.4±1.7*	55.2±2.1‡

Non-metabolized fraction, 9MPA fraction before β-oxidation; metabolized fraction, 9MPA fraction processed by β-oxidation. Other abbreviations see in Table 1.
**p<0.05 vs sham, ‡p<0.05 vs IR.*

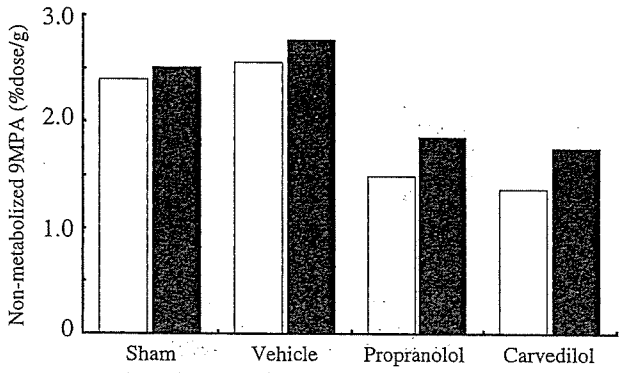

Fig 4. Amount of non-metabolized 9-methylpentadecanoic acid (9MPA) in the myocardium calculated from mean values of ^{131}I-9MPA accumulation in the ischemic (IR) and non-IR regions determined by autoradiography and the non-metabolized 9MPA fraction in the corresponding thin-layer chromatography study. (Open bars) IR; (solid bars) non-IR.

termined by dual-tracer autoradiography in each group and the non-metabolized 9MPA faction in the corresponding TLC study. As shown in Fig 4, the amount of non-metabolized 9MPA was decreased by carvedilol and propranolol in both the IR and non-IR.

Discussion

The major findings of the present study are as follows. First, a single administration of carvedilol before transient ischemia reduced myocardial 9MPA accumulation in both the IR and non-IR 3 days after reperfusion. Consequently, carvedilol did not affect a visual assessment of the autoradiographic image of 9MPA, but accelerated its clearance from both regions. Secondly carvedilol suppressed the intracellular accumulation of non-metabolized 9MPA, which implies that the administration of carvedilol before the onset of ischemia might have a beneficial effect on myocardial metabolism late in the reflow phase, because the accumulation of FA intermediates such as long-chain acyl-coenzyme A (CoA) and long-chain acylcarnitine has been implicated in the acceleration of ischemic heart failure[14–16] Finally, these effects of carvedilol were not different from those of propranolol, suggesting that the β-adrenoceptor blocking action of carvedilol might primarily contribute to alterations in cardiac FA metabolism.

Effects of β-Adrenoceptor Blockade on Cardiac FA Imaging

Branched-chain FA analogs such as ^{123}I-BMIPP and ^{123}I-9MPA are used clinically to assess FA metabolism in patients with coronary heart disease[2–6] Slow recovery of the tracer uptake after ischemic insult has been found in both clinical and experimental studies[17–19] In the present study, the reduced tracer uptake by the IR seen in the early image after tracer injection was not present in the delayed image because of slow clearance of the tracer in the IR, a finding consistent with the previous study[10]

Beta-adrenoceptor blockers, including carvedilol, are frequently prescribed for patients with coronary heart disease and heart failure, so it is important to clarify their influence on the distribution and intracellular metabolism of FA tracers in the myocardium. Miura et al reported that propranolol inhibited the myocardial accumulation of non-esterified FA in ischemic canine hearts using fluorescent labeling[20] In a study using positron emission tomography, carvedilol decreased the mean cardiac uptake rate of a long-chain FA tracer in patients with ischemic cardiomyopathy[21] In the present study, carvedilol suppressed myocardial accumulation of 9MPA in both the IR and non-IR and consequently, the autoradiographic images from hearts treated with carvedilol were visually similar to those from the vehicle group; that is, reduced accumulation of tracer in the IR in the early image and relatively homogeneous distribution of the tracer in the delayed image. These effects of carvedilol were not different from those of propranolol, suggesting the primary influence of β-adrenoceptor blocking action of carvedilol is on tracer kinetics, but not other mechanisms, such as α-blocking or antioxidant effects, that have been implicated previously[22,23] The present results also imply that the efficacy of cardiac FA imaging for the detection of coronary heart disease would not be decreased by treatment with β-blockers.

Effects of β-Blockade on Myocardial FA Metabolism After Ischemia-Reperfusion

Metabolism of ischemic tissue is characterized by decreased oxidation of long-chain FA with increased shunting of FA to TG. Myocardial ischemia causes augmentation of intramyocardial lipolysis, as well as increasing myocardial extraction of FA from blood because of the increased plasma concentration! Increased myocardial accumulation of acyl CoA may exert several deleterious effects, including uncoupling of oxidative phosphorylation, alteration of mitochondrial permeability, and impaired sarcolemmal function and intracellular Ca^{2+} handling![1,24] In the present study, the amount of non-metabolized 9MPA in the IR of the vehicle group did not decrease (Fig 4), despite a significant decrease in 9MPA accumulation assessed by autoradiography. These results suggest that no reduction in the level of acyl CoA in ischemia-reperfused myocardium may contribute to deterioration or slow recovery of myocardial function.

Reduction in myocardial 9MPA accumulation induced by carvedilol did not result from altered substrate availabili-

ty, because there were no significant changes in the plasma levels of FFA and glucose among the groups in the present study. Nanki et al showed that metoprolol inhibited the accumulation of acyl CoA in the mitochondria of ischemic myocardium[25] Panchal et al demonstrated a 28% decrease in the activity of myocardial carnitine palmitoyl transferase I (CPT-I), a key enzyme involved in mitochondrial FA uptake, after metoprolol treatment in dogs with coronary microembolization-induced heart failure[26] Moreover, DeGrado et al have clearly shown a marked reduction in myocardial accumulation of 14(R,S)-^{18}F-fluoro-6-thia-heptadecanoic acid in mice treated with the CPT-1 inhibitor[27] Thus, the decreased CPT-I activity by β-blockade may account for the reduction in myocardial FA accumulation, especially long-chain acyl CoA, after an ischemic insult.

Propranolol vs Carvedilol

Both propranolol and carvedilol are non-selective β-adrenoceptor blocking agents, but carvedilol has a α1-adrenoceptor blocking action and antioxidant property as well[22,23] In our preliminary study using sham-operated rats, the heart rate reduction induced by the present dose of carvedilol (1 mg/kg) was similar to that of propranolol (1 mg/kg) (19.0±8.9%, n=8 vs 18.5±8.0%, n=8). Therefore, the magnitude of β-blocking action of carvedilol might be equivalent to that of propranolol in the present study. The influence of carvedilol on 9MPA accumulation and its intracellular metabolism did not differ from that of propranolol. Taken together, alterations in myocardial FA metabolism by carvedilol might result primarily from its β-blocking property. In a recent study by Gambert et al[28] however, trimetazidine, an inhibitor of cardiac FA oxidation, improved postischemic mechanical dysfunction in association with reduced formation of free radicals in isolated rat hearts after reperfusion following 30-min global ischemia. They suggested that adverse effects of FAs on ischemia-reperfusion injury might be mediated, at least in part, by free radicals. In the present study, 15-min coronary occlusion followed by 3-day reperfusion did not result in macroscopic myocardial infarction, although we did not determine cardiac hemodynamics or oxidative stress. It remains unclear whether the antioxidant effects of carvedilol could attenuate myocardial ischemia-reperfusion injury in the heart after more prolonged coronary occlusion.

Study Limitations

Some methodologic limitations deserve comment. First, we did not determine whether β-adrenoceptor blockade might affect cardiac FA metabolism during ischemia or during reperfusion. Many factors could contribute to myocardial reperfusion injury, but free radical generation and intracellular Ca^{2+} overload are considered as major factors in reperfusion injury[29] Carvediolol has an antioxidant property, but its effect on 9MPA metabolism was not different from that of propranolol in the present study. Therefore, it seems likely that the β-blocking action of these drugs might affect cardiac metabolism during ischemia rather than during reperfusion. Second, effects of β-blockade on cardiac function were not evaluated in the present study. A 15-min coronary occlusion did not result in myocardial necrosis in our previous study[11] and rats treated with and without β-blockade did not show macroscopic myocardial infarction in the present study. However, β-blockade before ischemia might accelerate the recovery from myocardial stunning. Previous studies have shown that β-blockade reduced infarct size in the heart after more prolonged coronary occlusion[30,31] Further studies are required to investigate whether changes in FA metabolism by β-blockade may accelerate recovery from myocardial stunning.

Conclusions

The present study results indicate that β-adrenoceptor blockade does not affect the visual assessment of autoradiographic images of FA tracer in the rat heart after ischemia-reperfusion injury, suggesting that β-blockade does not affect the capability of FA tracer to detect coronary heart disease. Branched chain FA analogs are processed, at least in part, via α- and β-oxidation in the in-situ heart, and, therefore a dynamic study of FA tracer accumulation, including 9MPA and BMIPP, may provide useful information on intracellular FA metabolism.

References

1. Katz AM, Messineo FC. Lipid-membrane interaction and the pathogenesis of ischemic damage in the myocardium. *Circ Res* 1981; **48:** 1–16.
2. Knapp FF Jr, Goodman MM, Callahan PA, Kirsch G. Radioiodinated 15-(p-iodophenyl)-3,3-dimethylpentadecanoic acid: A useful new agent to evaluate myocardial fatty acid uptake. *J Nucl Med* 1986; **27:** 521–531.
3. Franken RP, Geeter DF, Dendale P, Demoor D, Block P, Bossuyt A. Abnormal free fatty acid uptake in subacute myocardial infarction after coronary thrombolysis: Correlation with wall motion and inotropic reserve. *J Nucl Med* 1994; **35:** 1758–1765.
4. Dilsizian V, Bateman TM, Bergmann SR, Prez RD, Magram MY, Goodbody AE, et al. Metabolic imaging with β-methyl-*p*-[^{123}I]-iodophenyl-pentadecanoic acid identifies ischemic memory after demand ischemia. *Circulation* 2005; **112:** 2169–2174.
5. Hashimoto J, Kubo A, Iwasaki R, Fujii H, Kunieda E, Iwanaga S, et al. Scintigraphic evaluation of myocardial ischemia using a new fatty acid analogue: Iodine-123-labelled 15-(p-iodophenyl)-9-(R,S)-methylpentadecanoic acid (9MPA). *Eur J Nucl Med* 1999; **26:** 887–893.
6. Fujiwara S, Takeishi Y, Tojo T, Yamaoka M, Nitobe J, Takeishi K, et al. Fatty acid imaging with 123-I-15-(p- iodophenyl)-9-R,S-methylpentadecanoic acid in acute coronary syndrome. *J Nucl Med* 1999; **40:** 1999–2006.
7. Tamaki N, Morita K, Kuge Y, Tsukamoto E. The role of fatty acids in cardiac imaging. *J Nucl Med* 2000; **41:** 1525–1534.
8. Yamamichi Y, Kusuoka H, Morishita K, Shirakami Y, Kurami M, Okano K, et al. Metabolism of iodine-123-BMIPP in perfused rat hearts. *J Nucl Med* 1995; **36:** 1043–1054.
9. Hosokawa R, Nohara R, Fujibayashi Y, Okuda K, Ogino M, Hata T, et al. Myocardial kinetics of iodine-123-BMIPP in canine myocardium after regional ischemia and reperfusion: Implications for clinical SPECT. *J Nucl Med* 1997; **37:** 1857–1863.
10. Igarashi N, Nozawa T, Fujii N, Kato B, Nonomura M, Matsuki A, et al. Evaluation of fatty acid metabolism in hearts after ischemia-reperfusion injury using a dual isotope autoradiographic approach and tissue assay for metabolites of tracer. *J Nucl Med* 2005; **46:** 160–164.
11. Kato B, Nozawa T, Igarashi N, Nonomura M, Fujii N, Igawa A, et al. Discrepant recovery course of sympathetic neuronal function and β-adrenoceptors in rat hearts after reperfusion following transient ischemia. *J Nucl Med* 2004; **45:** 1074–1080.
12. Folch J, Lees M, Stanley SH. A simple method for the isolation and purification of total lipids from animal tissues. *J Biol Chem* 1957; **226:** 497–509.
13. Fujii N, Nozawa T, Igawa A, Kato B, Igarashi N, Nonomura M, et al. Saturated glucose uptake capacity and impaired fatty acid oxidation in hypertensive hearts before development of heart failure. *Am J Physiol Heart Circ Physiol* 2004; **287:** H760–H766.
14. Liedtke AJ, Nellis S, Neely JR. Effects of excess free fatty acids on mechanical and metabolic function in normal and ischemic myocardium in swine. *Circ Res* 1978; **43:** 652–661.
15. Liu Q, Docherty JC, Rendell JC, Clanachan AS, Lopaschuk GD. High levels of fatty acids delay the recovery of intracellular pH and cardiac efficiency in post-ischemic hearts by inhibiting glucose oxidation. *J Am Coll Cardiol* 2002; **39:** 718–725.
16. Korge P, Honda HM, Weiss JN. Effects of fatty acids in isolated